VECTOR PENALTY-PROJECTION METHOD FOR INCOMPRESSIBLE FLUID FLOWS WITH OPEN BOUNDARY CONDITIONS

Philippe Angot, Rima Cheaytou

Proceedings of ALGORITMY 2012
pp. 219–229

VECTOR PENALTY-PROJECTION METHOD FOR INCOMPRESSIBLE FLUID FLOWS WITH OPEN BOUNDARY CONDITIONS

PHILIPPE ANGOT * AND RIMA CHEAYTOU †

Abstract. A new family of methods, the so-called vector penalty-projection methods ($VPP_{r,\varepsilon}$), were introduced recently by Angot et al. [1, 2] to compute the solution of unsteady incompressible fluid flows and to overcome most of the drawbacks of the usual incremental projection methods. In this work, we deal with the time-dependent incompressible Stokes equations with outflow boundary conditions using the present method. The spatial discretization is based on the finite volume scheme on a MAC staggered grid and the time discretization is based on the backward difference formula of second-order BDF2 (namely also Gear's scheme). We show that the ($VPP_{r,\varepsilon}$) method provides a second-order convergence for both velocity and pressure in space and time even in the presence of open boundary conditions with small values of the augmentation parameter r; typically $0 \leq r \leq 1$ and a penalty parameter ε small enough; typically $\varepsilon = 10^{-10}$. The resulting constraint on the discrete divergence of velocity is not exactly equal to zero but is satisfied approximately as $\mathcal{O}(\varepsilon\,\delta t)$ with a penalty parameter ε as small as desired. Finally, the efficiency and the second-order accuracy of our method are illustrated by several numerical cases.

Key words. Vector penalty-projection methods, Stokes equations, incompressible flows, open boundary conditions, second-order convergence.

AMS subject classifications. 35Q30, 35Q35, 49M30, 65M08, 65M85, 65N08, 65N85, 74F10, 76D05, 76D45, 76M12, 76R10, 76T10

1. Introduction.

The numerical solution of incompressible fluid flows has always been one of important subjects in fluid dynamics. The major difficulty in numerically solving unsteady incompressible Navier-Stokes equations in primitive variable form arises from the fact that the velocity and the pressure are coupled by the incompressibility constraint at each time step. There are numerous ways to discretize these equations. The most widespread methods are projection methods like pressure-correction methods. This family of methods has been introduced by Chorin and Temam [6, 14] in the late sixties. The interest of pressure-correction projection methods is that the velocity and the pressure are computed separately. Actually, in a first step, we solve the momentum balance equation to obtain an intermediate velocity and then, this intermediate velocity is projected on the space of solenoidal vector fields. Using this method, a numerical error named the splitting error appears and several papers have been written to estimate this error. In 1992, Shen [13] has introduced a modified approach which consists of adding in the first step of the scheme a penalty term built from the divergence constraint, it is the so-called penalty-projection method. In the same way, Jobelin et al. [10] proposed a numerical scheme which falls in the category of the penalty-projection method with an augmentation parameter $r \geq 0$ independent of the time step δt. Recently, Angot et al. [1] propose a new family of methods, the so-called two-parameters vector penalty-projection method $(VPP_{r,\varepsilon})_{r\geq 0, 0<\varepsilon\leq 1}$ (r and ε represent the augmentation parameter and the penalty

*Aix-Marseille Université, LATP - CMI, CNRS UMR7353, 13453 Marseille Cedex 13 - France. (angot@cmi.univ-mrs.fr).

†Aix-Marseille Université, LATP - CMI, CNRS UMR7353, 13453 Marseille Cedex 13 - France.(rima.cheaytou@gmail.com)

parameter respectively). Angot et al. have tested in [1, 2, 5] the $(VPP_{r,\varepsilon})$ method using a first-order scheme in time and in presence of Dirichlet boundary conditions. They found that the scheme is $\mathcal{O}(\delta t)$ in time for velocity and pressure. However, many applications such as free surface problems and channel flows have to deal with open boundary conditions on a part of the boundary which is still the challenging problem. Many recent progress were made in this direction including Guermond et al. [9], Jobelin et al. [10], Fevriére et al. [7], Liu [11] and Poux et al. [12].

The objective of the present work is to show the optimal convergence of the vector-penalty projection methods when solving the unsteady incompressible Stokes problems including open boundary conditions.

2. Formulation of the continuous problem. Let $\Omega \subset R^d$ ($d = 2$ or 3 in practice) be an open, bounded and connected domain with a Lipschitz continuous boundary $\Gamma = \partial\Omega$. We suppose that Γ is partitioned in two subsets Γ_D and Γ_N, of outward unit normal vector $\mathbf{n}$, such that $\Gamma = \Gamma_D \cup \Gamma_N$, $\Gamma_D \cap \Gamma_N = \emptyset$. The generic point of Ω is denoted $\mathbf{x}$. For $T > 0$, we consider the time-dependent Stokes equations governing incompressible fluid flow on a finite time interval [0,T] which read:

$$\rho\frac{\partial \mathbf{v}}{\partial t} - \mu\,\Delta\mathbf{v} + \nabla p = \mathbf{f} \ \text{ in } \Omega\times]0,T[\tag{2.1}$$

$$\nabla\cdot\mathbf{v} = 0 \quad \text{in } \Omega\times]0,T[\tag{2.2}$$

$$\mathbf{v} = \mathbf{v}_D \quad \text{on } \Gamma_D\times]0,T[\tag{2.3}$$

$$-\,p\,\mathbf{n} + \mu\,\nabla\mathbf{v}\cdot\mathbf{n} = \mathbf{g} \quad \text{on } \Gamma_N\times]0,T[\tag{2.4}$$

where $\mathbf{v}=(u,v)^T$ stands for the fluid velocity of initial value $\mathbf{v}(t=0) = \mathbf{v}_0$, p for the pressure field, ρ for the fluid density (the density is taken to be one), μ for the dynamic viscosity (here, $\mu = \frac{1}{Re}$ with Re a given Reynolds number). We impose Dirichlet boundary conditions (2.3) on Γ_D, and open boundary condition (2.4) on Γ_N. The external body forces $\mathbf{f}$, the pseudo-stress vector $\mathbf{g}$ and the Dirichlet boundary condition $\mathbf{v}_D$ are known.

Finally, the reader will keep in mind that bold letters like $\mathbf{v}$, $\mathbf{g}$, etc., indicate vector valued quantities.

3. Vector penalty-projection methods with open boundary condition. Let $0 = t^0 < t^1 < ... < t^N = T$ be a partition of the time interval of computation [0,T], which we suppose uniform for the sake of simplicity. We denote by δt the time step, i.e., the constant difference between two successive times t^n and t^{n+1}.

3.1. Description of the $(VPP_{r,\varepsilon})$ method with OBC (3.6). We describe now, the two-step vector penalty-projection method $(VPP_{r,\varepsilon})$ using OBC (3.6) as an open boundary condition in the projection step with an augmentation parameter $r \geq 0$ and a penalty parameter $0 < \varepsilon \ll 1$.

3.1.1. BDF2 time scheme. For all $n \geq 1$ such that $(n+1)\delta t \leq T$ and for $\widetilde{\mathbf{v}}^0, \widetilde{\mathbf{v}}^1, \mathbf{v}^0, \mathbf{v}^1 \in \mathbf{L}^2(\Omega)$ and $p^0, p^1 \in L^2_0(\Omega)$ given, find $(\mathbf{v}^{n+1}, p^{n+1})$ such that:

- **Vector penalty-prediction step with an augmentation parameter** $r \geq 0$:

$$\frac{3\widetilde{\mathbf{v}}^{n+1}-4\widetilde{\mathbf{v}}^{n}+\widetilde{\mathbf{v}}^{n-1}}{2\delta t}-\mu\,\Delta\widetilde{\mathbf{v}}^{n+1}-r\,\nabla(\nabla\cdot\widetilde{\mathbf{v}}^{n+1})+\nabla p^{\star,n+1}=\mathbf{f}^{n+1}\ \text{ in }\Omega \tag{3.1}$$

$$\widetilde{\mathbf{v}}^{n+1}=\mathbf{v}_D^{n+1}\quad\text{on }\Gamma_D \tag{3.2}$$

$$(-p^{\star,n+1}+r\,\nabla\cdot\widetilde{\mathbf{v}}^{n+1})\,\mathbf{n}+\mu\,\nabla\widetilde{\mathbf{v}}^{n+1}\cdot\mathbf{n}=\mathbf{g}^{n+1}\text{on }\Gamma_N \tag{3.3}$$

where $p^{\star,n+1}=2p^n-p^{n-1}$ (by a second-order Richardson's extrapolation)

- **Vector penalty-projection step with a penalty parameter** $0<\varepsilon\leq 1$:

$$\frac{3\widehat{\mathbf{v}}^{n+1}-4\widehat{\mathbf{v}}^{n}+\widehat{\mathbf{v}}^{n-1}}{2\delta t}-\varepsilon\,\mu\,\Delta\widehat{\mathbf{v}}^{n+1}-\frac{1}{\varepsilon}\,\nabla\left(\nabla\cdot\widehat{\mathbf{v}}^{n+1}\right)=\frac{1}{\varepsilon}\nabla\left(\nabla\cdot\widetilde{\mathbf{v}}^{n+1}\right)\text{ in }\Omega \tag{3.4}$$

$$\widehat{\mathbf{v}}^{n+1}=0\quad\text{on }\Gamma_D \tag{3.5}$$

$$\mu\,\nabla\widehat{\mathbf{v}}^{n+1}\cdot\mathbf{n}=0\ \text{ on }\Gamma_N\quad\text{(OBC)} \tag{3.6}$$

- **Correction step for velocity and pressure**:

$$\mathbf{v}^{n+1}=\widetilde{\mathbf{v}}^{n+1}+\widehat{\mathbf{v}}^{n+1} \tag{3.7}$$

$$p^{n+1}=2p^n-p^{n-1}-\frac{1}{\varepsilon}\,(\nabla\cdot\mathbf{v}^{n+1})-r\,\nabla\cdot\widetilde{\mathbf{v}}^{n+1} \tag{3.8}$$

Remark 1. *Summing the prediction and projection steps gives the discrete problem which is effectively solved by the above splitting scheme:*

$$\begin{aligned}
&\frac{3\boldsymbol{v}^{n+1}-4\boldsymbol{v}^{n}+\boldsymbol{v}^{n-1}}{2\delta t}-\mu\,(\Delta\widetilde{\boldsymbol{v}}^{n+1}+\varepsilon\,\Delta\widehat{\boldsymbol{v}}^{n+1})+\nabla p^{n+1}=\boldsymbol{f}^{n+1} && \text{in }\ \Omega\times]0,T[\\
&(\varepsilon\delta t)\frac{p^{n+1}-p^{\star,n+1}}{\delta t}+\nabla\cdot\boldsymbol{v}^{n+1}+r\,\varepsilon\,\nabla\cdot\widetilde{\boldsymbol{v}}^{n+1}=0 && \text{in }\Omega\times]0,T[\\
&\boldsymbol{v}^{n+1}=\boldsymbol{v}_D^{n+1} && \text{on }\Gamma_D\times]0,T[\\
&(-p^{\star,n+1}+r\,\nabla\cdot\widetilde{\boldsymbol{v}}^{n+1})\,\boldsymbol{n}+\mu\,\nabla\boldsymbol{v}^{n+1}\cdot\boldsymbol{n}=\boldsymbol{g}^{n+1} && \text{on }\Gamma_N\times]0,T[
\end{aligned}$$

As a consequence of the previous system, one would note that the $(VPP_{r,\varepsilon})$ *method lost a little consistency. Nevertheless, the method can be ultra-fast and very cheap if* $\eta=\varepsilon/\delta t$ *is sufficiently small due to the adapted right hand-side in the correction step which lies in the range of the left hand side as* ε *is taken small enough. This crucial property was already shown in [5, Theorem 1.1 and Corollary 1.3] and in [4, Theorem 3.1] and numerically confirmed also in [4, 5].*

3.1.2. Correction of pressure gradient for $r=0$ and small values of ε. The augmentation parameter r in our method is kept constant and within small values ($0\leq r\leq 1$) to avoid to excessively degrade the conditioning of the linear system associated to the prediction step. However, taking $r=0$, we obtain a poor convergence convergence rate in time for velocity and pressure: see the numerical results in Section 4. To improve the convergence rate, we reconstruct the pressure field itself very fast from its gradient as already proposed by Angot et al. in [3, 2, 5] where they observed that it is numerically far better to update directly the pressure gradient to avoid the effect of round-off errors when ε is very small.

In this regard, the updating of the pressure in our method is as follows:

Taking the gradient of the equation (3.8), we get:

$$\nabla p^{n+1} = 2\nabla p^n - \nabla p^{n-1} - \frac{1}{\varepsilon}\nabla(\nabla\cdot\mathbf{v}^{n+1}) - r\,\nabla(\nabla\cdot\widetilde{\mathbf{v}}^{n+1}) \tag{3.9}$$

Moreover, we have the following equality in the penalty-projection step:

$$\frac{3\widehat{\mathbf{v}}^{n+1} - 4\widehat{\mathbf{v}}^n + \widehat{\mathbf{v}}^{n-1}}{2\delta t} - \varepsilon\,\mu\,\Delta\widehat{\mathbf{v}}^{n+1} = \frac{1}{\varepsilon}\nabla(\nabla\cdot\mathbf{v}^{n+1})$$

Now, replacing the term , $\frac{1}{\varepsilon}\nabla(\nabla\cdot\mathbf{v}^{n+1})$ in (3.9) by the term deduced from the above equality. It yields the estimation of the gradient of the pressure:

$$\nabla p^{n+1} = 2\nabla p^n - \nabla p^{n-1} - \frac{3\widehat{\mathbf{v}}^{n+1} - 4\widehat{\mathbf{v}}^n + \widehat{\mathbf{v}}^{n-1}}{2\delta t} + \varepsilon\,\mu\,\Delta\widehat{\mathbf{v}}^{n+1} - r\,\nabla(\nabla\cdot\widetilde{\mathbf{v}}^{n+1}) \quad \text{with } r \geq 0 \tag{3.10}$$

3.2. Description of $(VPP_{r,\varepsilon})$ method with OBC1 (3.16). The $(VPP_{r,\varepsilon})$ method with OBC (3.6) yields good numerical results (see Section 4). However, we observe that the well-posedness of the penalty-projection step using OBC (3.6) is not straightforward. Thus, we propose to replace OBC (3.6) by OBC1 (3.16) which clearly yields a well-posed penalty-projection step (see Lemma 3.1).

3.2.1. BDF2 time scheme. For all $n \geq 1$ such that $(n+1)\delta t \leq T$ and for $\widetilde{\mathbf{v}}^0$, $\widetilde{\mathbf{v}}^1$,$\mathbf{v}^0$, $\mathbf{v}^1 \in \mathbf{L}^2(\Omega)$ and $p^0, p^1 \in L^2_0(\Omega)$ given, find $(\mathbf{v}^{n+1}, p^{n+1})$ such that:

- **Vector penalty-prediction step with an augmentation parameter** $r \geq 0$:

$$\frac{3\widetilde{\mathbf{v}}^{n+1} - 4\widetilde{\mathbf{v}}^n + \widetilde{\mathbf{v}}^{n-1}}{2\delta t} - \mu\Delta\widetilde{\mathbf{v}}^{n+1} - r\nabla(\nabla\cdot\widetilde{\mathbf{v}}^{n+1}) + \nabla p^{\star,n+1} = \mathbf{f}^{n+1} \text{ in } \Omega \tag{3.11}$$

$$\widetilde{\mathbf{v}}^{n+1} = \mathbf{v}_D \ \text{ on } \Gamma_D \tag{3.12}$$

$$(-p^{\star,n+1} + r\nabla\cdot\widetilde{\mathbf{v}}^{n+1})\mathbf{n} + \mu\nabla\widetilde{\mathbf{v}}^{n+1}\cdot\mathbf{n} = \mathbf{g}^{n+1} \ \text{ on } \Gamma_N \tag{3.13}$$

where $p^{\star,n+1} = 2p^n - p^{n-1}$ (by a second-order Richardson's extrapolation)

- **Vector penalty-projection step with a penalty parameter** $0 < \varepsilon \leq 1$:

$$\frac{3\widehat{\mathbf{v}}^{n+1} - 4\widehat{\mathbf{v}}^n + \widehat{\mathbf{v}}^{n-1}}{2\delta t} - \varepsilon\mu\Delta\widehat{\mathbf{v}}^{n+1} - \frac{1}{\varepsilon}\nabla\left(\nabla\cdot\widehat{\mathbf{v}}^{n+1}\right) = \frac{1}{\varepsilon}\nabla\left(\nabla\cdot\widetilde{\mathbf{v}}^{n+1}\right) \text{ in } \Omega \tag{3.14}$$

$$\widehat{\mathbf{v}}^{n+1} = 0 \ \text{ on } \Gamma_D \tag{3.15}$$

$$\widehat{\mathbf{v}}^{n+1}\cdot\mathbf{n} = 0 \quad \text{and} \quad (\mu\nabla\widehat{\mathbf{v}}^{n+1}\cdot\mathbf{n}) \wedge \ \mathbf{n} = 0 \ \ \text{(OBC1)} \ \text{ on } \Gamma_N \tag{3.16}$$

- **Correction step for velocity and reconstruction of the pressure from its gradient**:

$$\mathbf{v}^{n+1} = \widetilde{\mathbf{v}}^{n+1} + \widehat{\mathbf{v}}^{n+1}$$

$$\nabla p^{n+1} = 2\nabla p^n - \nabla p^{n-1} - \frac{3\widehat{\mathbf{v}}^{n+1} - 4\widehat{\mathbf{v}}^n + \widehat{\mathbf{v}}^{n-1}}{2\delta t} + \varepsilon\,\mu\Delta\widehat{\mathbf{v}}^{n+1} - r\nabla(\nabla\cdot\widetilde{\mathbf{v}}^{n+1})$$

Remark 2. *For any vector $\boldsymbol{u} \in R^d$ defined on Γ, the tangential component $\boldsymbol{u}\bigwedge\boldsymbol{n}|_\Gamma$ is defined by: $\boldsymbol{u}\bigwedge\boldsymbol{n}|_\Gamma = \boldsymbol{u}_\tau\bigwedge\boldsymbol{n}|_\Gamma$ with $\boldsymbol{u}_\tau = \boldsymbol{u} - (\boldsymbol{u}\ \cdot\ \boldsymbol{n})\boldsymbol{n}$. Thus, in 2-D (d*

= 2), we have simply: $\boldsymbol{u} \bigwedge \boldsymbol{n}|_\Gamma = u \cdot \tau$*, where* τ *denotes a unit tangential vector on* Γ*.*

LEMMA 3.1. ***(Well-posedness of the velocity correction step (3.14-3.16))*** *For all* $\widetilde{\boldsymbol{v}}^{n+1}$ *given in* $\boldsymbol{H}^1(\Omega)$ *and for all* $\varepsilon > 0$ *and* $\delta t > 0$*, there exists at each time step a unique solution* $\widehat{\boldsymbol{v}}^{n+1} \in \boldsymbol{W}(\Omega)$ *to the velocity-correction step (3.14-3.16), where* $\boldsymbol{W}(\Omega) = \left\{ \boldsymbol{u} \in \boldsymbol{H}^1(\Omega)^d;\ \boldsymbol{u} = 0\ on \Gamma_D \text{ and } \boldsymbol{u} \cdot \boldsymbol{n} = 0\ on \Gamma_N \right\}$ *is an Hilbert space.*

SKETCH OF PROOF.

For sake of simplicity, we take the discrete form of projection step and we use Euler scheme to discretize in time. Multiplying the projection step by a test function $\varphi \in \mathbf{W}(\Omega)$ and applying the Green formula, we obtain the following bilinear form: $a(\widehat{\mathbf{v}}, \varphi) = \frac{\varepsilon}{\delta t}(\widehat{\mathbf{v}}, \varphi)_0 + \varepsilon^2 \mu (\nabla \widehat{\mathbf{v}}, \nabla \varphi)_0 + (\nabla \cdot \widehat{\mathbf{v}}, \nabla \cdot \varphi)_0$ in $\mathbf{W}(\Omega) \times \mathbf{W}(\Omega)$. We note that $a(\widehat{\mathbf{v}}, \varphi)$ is a continuous and coercive form in $\mathbf{W}(\Omega) \times \mathbf{W}(\Omega)$ and $L(\varphi) := (\nabla \cdot \widetilde{\mathbf{v}}, \nabla \cdot \varphi)_0$ is a linear continuous form in $\mathbf{W}(\Omega)$. Under these hypotheses, we can easily apply Lax-Milgram theorem which ensures that the penalty-projection step is well-posed and admits a unique solution $\widehat{\mathbf{v}}^{n+1}$ in the Hilbert space $\mathbf{W}(\Omega)$ equipped with the usual norm of $\mathbf{H}^1(\Omega)$.

4. Numerical experiments. We consider the unit square as our computation domain $\Omega =]0, 1[^2$. The Dirichlet condition is prescribed on $\partial\Omega$, except for the part included in the y-axis, where the open boundary conditions (2.4) are imposed. We present hereafter a convergence study for two manufactured test cases with an open boundary condition, homogeneous or not.

4.1. Homogeneous outflow boundary conditions ($g = 0$). We choose a test case already used in the literature [9, 10]. It consists in unstationary Stokes problem, with a forcing term and initial and boundary conditions corresponding to the following expression for the velocity and pressure:

$$\begin{aligned} u(x, y, t) &= \sin(x)\ \sin(y + t) \\ v(x, y, t) &= \cos(x)\ \cos(y + t) \\ p(x, y, t) &= \cos(x)\ \sin(y + t) \end{aligned}$$

Convergence rate in space We are interested to study the space convergence rate for Stokes equations with open boundary conditions. In order to estimate the spatial error, we focus on the stationary solution of the above numerical experiment. We fix the time step at a small value: $\delta t = 10^{-2}$, the penalty parameter ε at 10^{-10}, the augmentation parameter r at 10^{-4} and we run the algorithm for different values of the spatial mesh step h.

The convergence rate of the error on velocity and pressure is around $\mathcal{O}(h^2)$ (see Figs. 4.1 and 4.2).

As a conclusion on the spatial convergence rate, we can say that the results obtained here conform with those reported by Poux et al. [12]. Besides, the $(VPP_{r,\varepsilon})$ method appears more accurate than the standard incremental scheme studied by Guermond et al. [9]. Particularly, our method improves the spatial convergence from $\mathcal{O}(h)$ to $\mathcal{O}(h^2)$ for the velocity and from $\mathcal{O}(h^{1/2})$ to $\mathcal{O}(h^2)$ for pressure.

Convergence rate in time We consider the unsteady homogeneous case. The convergence tests with respect to δt are reported in Figs 4.3 and 4.4. The convergence rate of the error on the velocity in the L^2-norm is close to $\mathcal{O}(\delta t^2)$. The situation is somewhat similar for the pressure. The convergence results for this quantity in L^2-norm seem to behave like $\mathcal{O}(\delta t^2)$. These rates seem similar to those obtained by

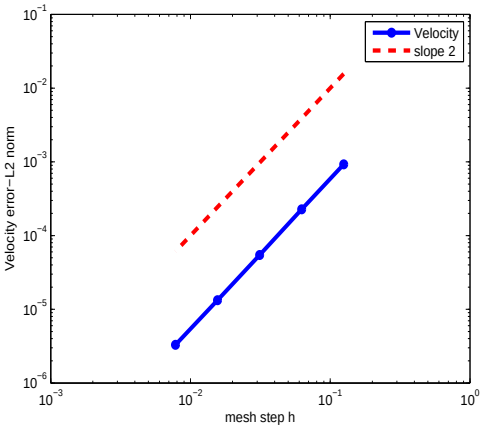

FIG. 4.1. *Homogeneous open boundary condition - OBC - Velocity error L^2-norm versus mesh step at T=2, δt=10^{-2}, ε=10^{-10}, $r = 10^{-4}$.*

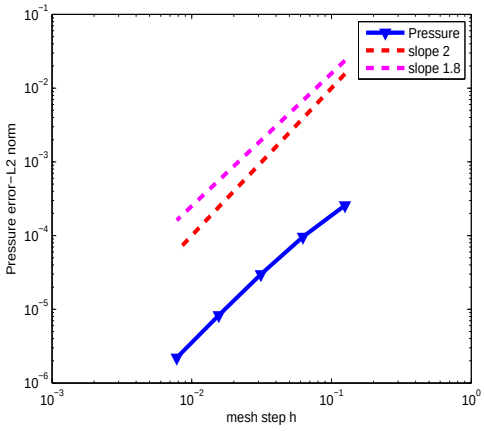

FIG. 4.2. *Homogeneous open boundary condition - OBC - Pressure error L^2-norm versus mesh step at T=2, δt=10^{-2}, ε=10^{-10}, $r = 10^{-4}$.*

Poux et al [12] in the rotational form of their method. Also, the errors of velocity and pressure for the $(VPP_{r,\varepsilon})$ method seem to be smaller than that computed in [12] even if the mesh we have used is coarser. Moreover, the $(VPP_{r,\varepsilon})$ methods improves the poor convergence rates of the standard BDF2 pressure-correction [8] scheme from $\mathcal{O}(\delta t)$ to $\mathcal{O}(\delta t^2)$ for the velocity and from $\mathcal{O}(\delta t^{1/2})$ to $\mathcal{O}(\delta t^2)$ for the pressure. Indeed, in [8], the second-order rotational pressure-correction yields $\mathcal{O}(\delta t^{3/2})$ accuracy for the velocity in the L^2-norm and $\mathcal{O}(\delta t)$ accuracy for the pressure.

It is useful to note that we checked numerically the value of $\widehat{\mathbf{v}} \cdot \mathbf{n}$ on the boundary Γ_N in the projection step using $(VPP_{r,\varepsilon})$ method with OBC (3.6). We obtain that $\widehat{\mathbf{v}} \cdot \mathbf{n}$ is of order 10^{-12} so, practically equal to zero.

Besides, Fig. 4.5 shows the L^2-norm of the velocity divergence as a function of epsilon. We find that the constraint on the discrete velocity divergence is satisfied approximately as $\mathcal{O}(\varepsilon\delta t)$ with $0 < \varepsilon \leq 1$ a small as desired. Moreover, in Fig. 4.6, we plot the L^2-norm of the velocity divergence as a function of the time step δt. We obtain that the velocity divergence varies like $\mathcal{O}(\varepsilon\, \delta t)$ for ε quite small.

Finally, in order to check also the $(VPP_{r,\varepsilon})$ method using OBC1 (3.16) in the projection step, we simulate numerically the same test case already done. Figs. 4.7 and 4.8 display the errors of the computed velocity and gradient pressure in the L^2-norm for $\varepsilon = 10^{-10}$ and $r = 0$. The numerical results show that a 2nd order accuracy in time is recovered for both velocity and gradient pressure.

Convergence rate in time at $r = 0$ ***for the*** $(VPP_{r,\varepsilon})$ ***method with OBC (3.6) with the pressure gradient in (3.10)*** We treat now the temporal convergence of the velocity and pressure in the case when $r = 0$ and $\varepsilon \ll 1$. For this purpose, we use BDF2 scheme for discretization in time, the open boundary condition OBC (3.6) in the projection step and we take the same above test. Fig. 4.9 displays the errors of the computed velocity in the L^2-norm for $r = 0$ and $\varepsilon = 10^{-10}$. The second-order convergence rate is not clearly observed contrary to the cases when $10^{-4} \leq r \leq 1$. Unfortunately, the slope of the velocity-error appears to be rather of first order. For the considered case also, Fig. 4.11 shows the distribution of the pressure error (using

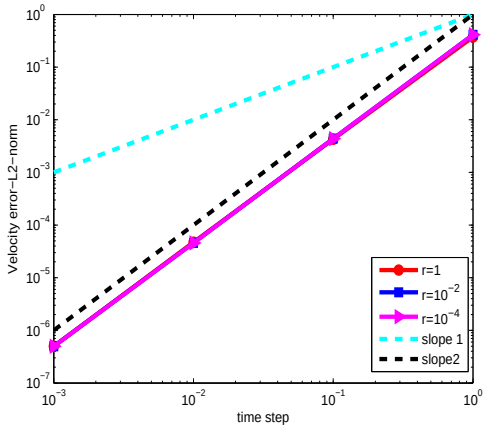

FIG. 4.3. *Homogeneous open boundary condition - OBC - Velocity error L^2-norm versus time step at T=2, mesh size:* $1/h = 128$, ε=10^{-10}.

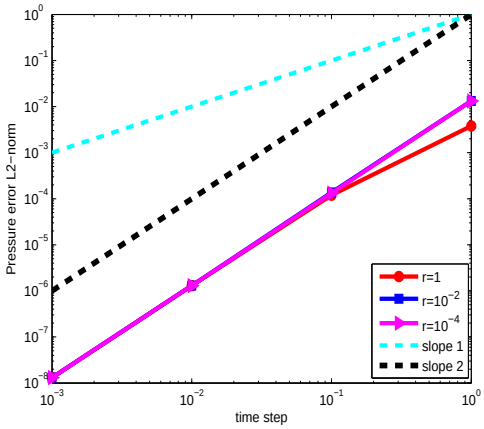

FIG. 4.4. *Homogeneous open boundary condition - OBC - Pressure error L^2-norm versus time step at T=2, mesh size:* $1/h = 128$, ε=10^{-10}.

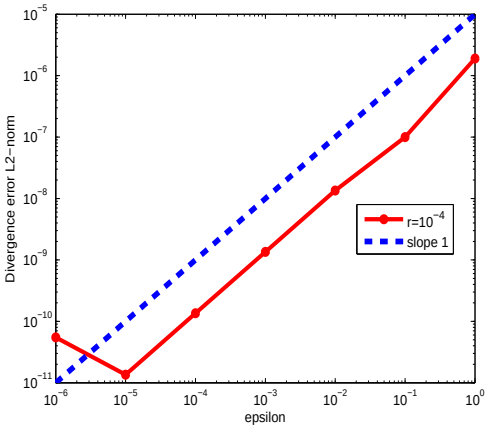

FIG. 4.5. *Homogeneous open boundary condition - OBC - Velocity divergence L^2-norm versus ε at T=2, mesh size:* $1/h = 128$, $r = 10^{-4}$.

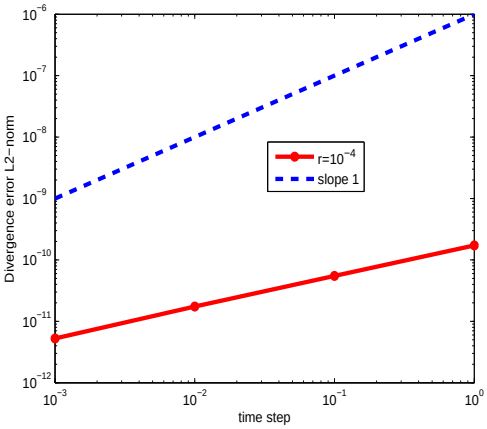

FIG. 4.6. *Homogeneous open boundary condition - OBC - Velocity divergence L^2-norm versus time step at T=2, mesh size:* $1/h = 128$, ε=10^{-6}.

(13)). As expected, the behavior of the pressure error in L^2-norm is strongly affected; we observe a sharp degradation of the pressure convergence (order 1/2 only) compared to the case when $10^{-4} \leq r \leq 1$. In fact, this deterioration of the convergence rate is due to the cumulation of round-off errors when ε is small enough.

Using the improvement of pressure explained in Section. 3.1.2, we repeat the same tests for $r = 0$. Fig. 4.10 presents the errors of the velocity in the L^2-norm. The velocity exhibits now a second-order convergence rate in time as well as in the case when $10^{-4} \leq r \leq 1$. In Fig. 4.12, the pressure gradient field achieves successfully 1.8th-order rate of convergence. These good results confirm the interest of updating the pressure by its gradient and provide a second-order convergence in time for $r \geq 0$

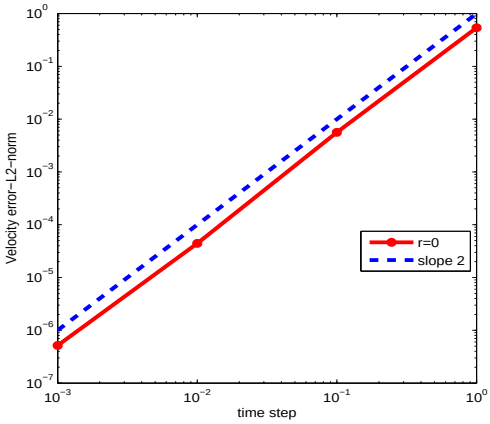

FIG. 4.7. *Homogeneous open boundary condition-OBC1-Velocity error L^2-norm versus time step at mesh size:* $1/h = 128$, ε=10^{-10}, $r = 0$.

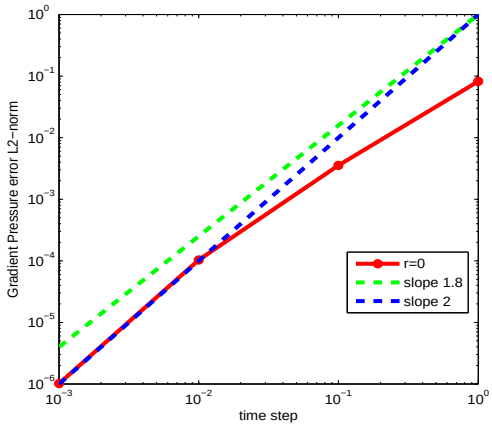

FIG. 4.8. *Homogeneous open boundary condition-OBC1-Gradient Pressure error L^2-norm versus time step at mesh size:* $1/h = 128$, ε=10^{-10}, $r = 0$.

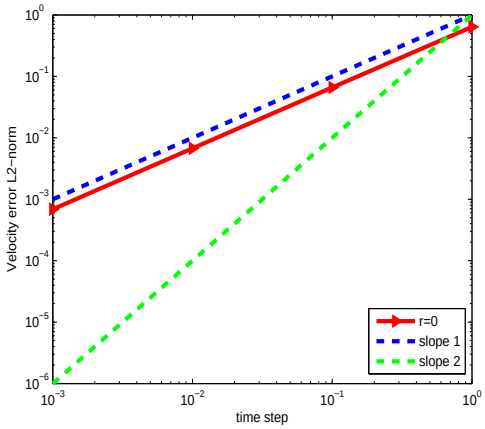

FIG. 4.9. *Homogeneous open boundary condition - OBC - Velocity error L^2-norm versus time step with standard pressure correction (3.8) at mesh size:* $1/h = 128$, $r = 0$, ε=10^{-10}.

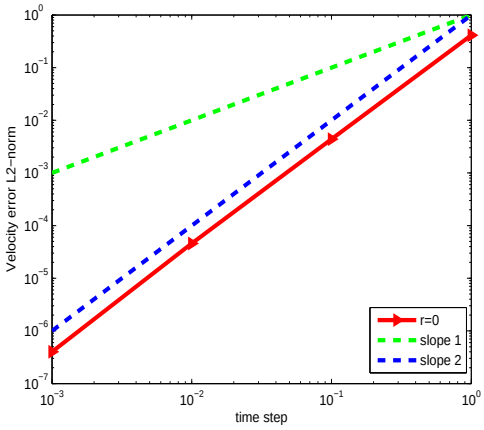

FIG. 4.10. *Homogeneous open boundary condition - OBC - Velocity error L^2-norm versus time step with the pressure gradient correction (3.10) at mesh size:* $1/h = 128$, $r = 0$, ε=10^{-10}.

which is in agreement with [3].

4.2. Nonhomogeneous outflow boundary conditions ($g \neq 0$). To further assess the influence of open boundary condition on the accuracy of the BDF2 vector penalty-projection methods, we have performed convergence tests with the

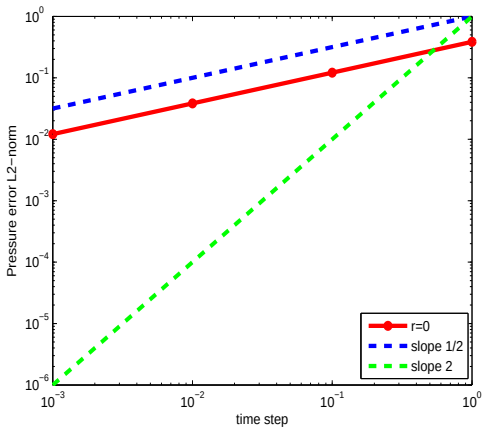

FIG. 4.11. *Homogeneous open boundary condition - OBC - Pressure error L^2-norm versus time step with standard pressure correction (3.8) at mesh size:* $1/h = 128$, ε=10^{-10}.

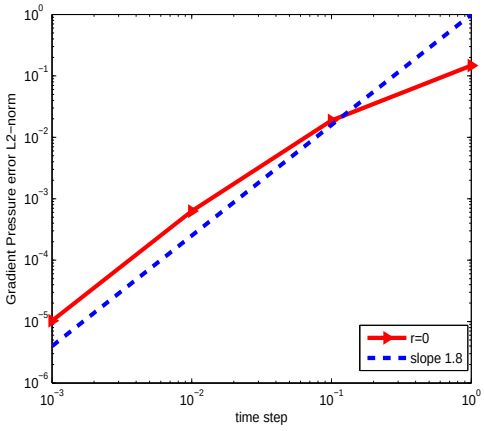

FIG. 4.12. *Homogeneous open boundary condition - OBC - Gradient pressure error L^2-norm versus time step with the pressure gradient correction (3.10) at mesh size:* $1/h = 128$, ε=10^{-10}.

nonhomogeneous case. For this aim, we take the same problem as in [11, 12]:

$$u(x,y,t) = \cos^2(\frac{\pi x}{2})\,\sin(\pi y)\,\cos(2\pi\omega t)$$
$$v(x,y,t) = -\cos^2(\frac{\pi y}{2})\,\sin(\pi x)\,\cos(2\pi\omega t)$$
$$p(x,y,t) = \cos(\frac{\pi x}{2})\,\sin(\frac{\pi y}{2})\,\cos(2\pi\omega t)$$

Convergence rate in time In the computations reported herein, we use the $(VPP_{r,\varepsilon})$ method with OBC (3.6). The curves are drawn for $\omega = 1$, $\varepsilon = 10^{-10}$ and different values of the augmentation parameter r; $10^{-4} \leq r \leq 1$. As one can see in Figs. 4.13 and 4.14, a convergence rate of order $\mathcal{O}(\delta t^2)$ is approximately observed for velocity and pressure. These results are in agreement with those reported in [12]. Indeed, it seems that the velocity divergence is almost of order $(\varepsilon\,\delta t)$ for ε small enough. The results are not shown here for sake of shortness.

We have also tested the convergence rate of velocity and gradient pressure using $(VPP_{r,\varepsilon})$ method with OBC1 (3.16). The results ensure also a second-order convergence for both unknowns (the results are not shown for brevity).

5. Conclusions. In this work, we have extended the vector penalty-projection $(VPP_{r,\varepsilon})$ method to the case of incompressible viscous flows with open boundary conditions. The numerical experiments reported here show that the $(VPP_{r,\varepsilon})$ method yields a considerable gain in accuracy compared to incremental pressure-correction scheme as well as in the standard form as rotational form [8] with small values of the augmentation parameter r; typically $0 \leq r \leq 1$ and a penalty parameter ε small enough. We also show that using the BDF2 second-order scheme for time discretization, the $(VPP_{r,\varepsilon})$ method yields $\mathcal{O}(\delta t^2)$ accuracy for velocity and pressure as well as in the homogeneous and nonhomogeneous open boundary conditions. Besides, the loss of spatial convergence in case of open boundary conditions does not occur anymore with our method. In fact, we obtain $\mathcal{O}(h^2)$ convergence in the L^2-norm of the

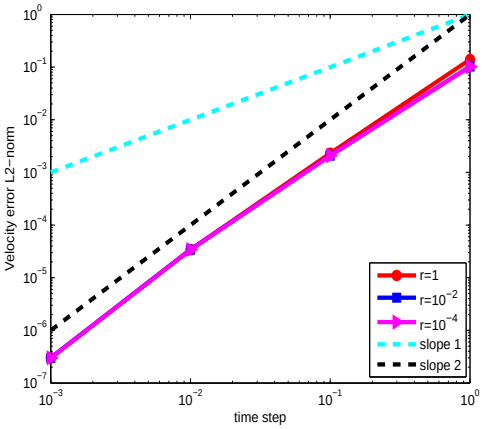

FIG. 4.13. *Nonhomogeneous open boundary condition - OBC - Velocity error L^2-norm versus time step at $T = 2$, mesh size:* $1/h = 128$, ε=10^{-10}.

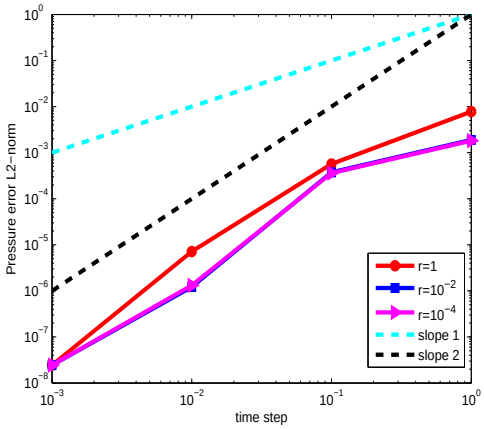

FIG. 4.14. *Nonhomogeneous open boundary condition - OBC - Pressure error L^2-norm versus time step at $T = 2$, mesh size:* $1/h = 128$, ε=10^{-10}.

velocity and pressure. The price to pay in the present method is that the constraint on the discrete divergence of velocity is not exactly equal to zero, but is satisfied approximately as $\mathcal{O}(\varepsilon\,\delta t)$ with a penalty parameter ε as small as desired up to machine precision. Finally, this method proves to be really efficient since it is fast, cheap, and provides very accurate results with an optimal spatial and temporal convergence despite the existence of outflow boundary conditions whereas other famous methods don't reach the same high convergence rate.

REFERENCES

[1] PH. ANGOT AND J.-P. CALTAGIRONE AND P. FABRIE, *Vector penalty-projection methods for the solution of unsteady incompressible flows*, Finite Volumes for Complex Applications V, (eds R. Eymard and J.-M. Herard), ISTE Ltd and J. Wiley and Sons, 59 (2008), pp. 169–176.

[2] PH. ANGOT AND J.-P. CALTAGIRONE AND P. FABRIE, *A spectacular vector penalty-projection method for Darcy and Navier-Stokes problems, in:*, J. Fort, et al.(Eds.), Finite Volumes for Complex Applications VI- Problems and Perspectives, in: Springer Proceedings in Mathematics 4, vol.1, Springer-Verglas, Berlin, (2011).

[3] PH. ANGOT AND J.-P. CALTAGIRONE AND P. FABRIE, *A fast vector penalty-projection method for incompressible Darcy and multiphase Navier-Stokes problems*, Nümerische Mathematik (submitted), (2011).

[4] PH. ANGOT AND J.-P. CALTAGIRONE AND P. FABRIE, *A fast vector penalty-projection method for incompressible non-homogeneous or multiphase Navier-Stokes problems*, Applied Mathematics Letters (in press), doi: 10.1016/ j.aml.2012.01.037, (2012).

[5] PH. ANGOT AND J.-P. CALTAGIRONE AND P. FABRIE, *A new fast method to compute saddle-points in constrained optimization and applications*, Applied Mathematics Letters, 25 (2012), pp. 245–251.

[6] A.J. CHORIN, *Numerical solution of the Navier-Stokes equationss*, Mathematics of Computation, 22 (1968), pp. 745–762.

[7] C. FÉVRIÈRE AND J. LAMINIE AND P. POULLET AND PH. ANGOT, *On the penalty-projection method for the Navier-Stokes equations with the MAC mesh*, J. Comput. Appl. Math., 226 (2009), pp. 228–245.

[8] J. L.GUERMOND AND J. SHEN, *On the error estimates for the rotational pressure-correction projection methods*, Math. Comp., 73 (2004), pp. 1719–1737 (electronic).

[9] J.L. Guermond and P. Minev and J. Shen, *An overview of projection methods for incompressible flows*, Comput. Methods Appl. Mech. Engrg., 195 (2006), pp. 6011–6045.

[10] M. Jobelin and C. Lapuerta and J.C Latché and Ph. Angot and B. Piar, *A finite element penalty-projection method for incompressible flows*, J. Comput. Phys., 217 (2006), pp. 502–518.

[11] J. Liu, *Open and traction boundary conditions for the incompressible Navier-Stokes equations*, Journal of Computational Physics, 228 (2009), pp. 7250–7267.

[12] A. Poux and S. Glockner and M. Azaïez, *Improvements on open and traction boundary conditions for Navier-Stokes time-splitting methods*, J. Comput. Phys., 230 (2011), pp. 4011–4027.

[13] J. Shen, *On error estimates of some higher order projection and penalty-projection methods for Navier-Stokes equations*, Numerische Mathematik, 62 (1992), pp. 49–74.

[14] R. Temam, *Sur l'approximation de la solution des équations de Navier-Stokes par la méthode des pas fractionnaires (II)*, Arch. Rational Mech. Anal., 33 (1969), pp. 377–385.